

**One-pot growth of triangular SnS nanopyramids for photoacoustic imaging and photothermal ablation of tumor**

Dongliang Yang<sup>1,2‡</sup>, Fei Chen<sup>3‡</sup>, Shili He<sup>3</sup>, Haifeng Shen<sup>3</sup>, Yanling Hu<sup>2,4</sup>, Ning Feng<sup>2</sup>, Siyu Wang<sup>2</sup>, Lixing Weng<sup>5</sup>, Zhimin Luo<sup>2</sup>, and Lianhui Wang<sup>2</sup>

<sup>1</sup> School of Physical and Mathematical Sciences, Nanjing Tech University (NanjingTech), 30 South Puzhu Road, Nanjing 211816, China.

<sup>2</sup> Key Laboratory for Organic Electronics and Information Displays and Jiangsu Key Laboratory for Biosensors, Institute of Advanced Materials (IAM), Jiangsu National Synergetic Innovation Center for Advanced Materials (SICAM), Nanjing University of Posts and Telecommunications, 9 Wenyuan Road, Nanjing 210023, China.

<sup>3</sup> Laboratory of Polymer Materials and Engineering, Ningbo Institute of Technology, Zhejiang University, Ningbo 315100, China.

<sup>4</sup> School of Electrical and Control, Nanjing Polytechnic Institute, No.625, Geguan Road, Nanjing City, 210048, Jiangsu, China.

<sup>5</sup> College of Geography and Biological Information, Nanjing University of Posts and Telecommunications, 9 Wenyuan Road, Nanjing 210023, China.

‡ These authors contributed equally to this article.

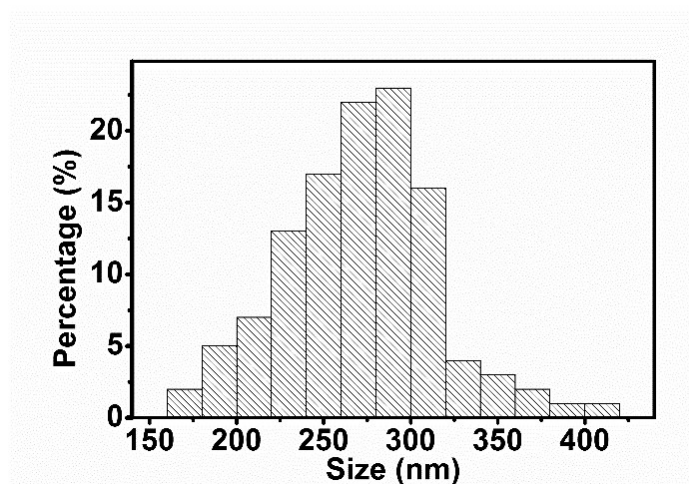


Fig S1. Size distribution of SnS nanopyrramids.

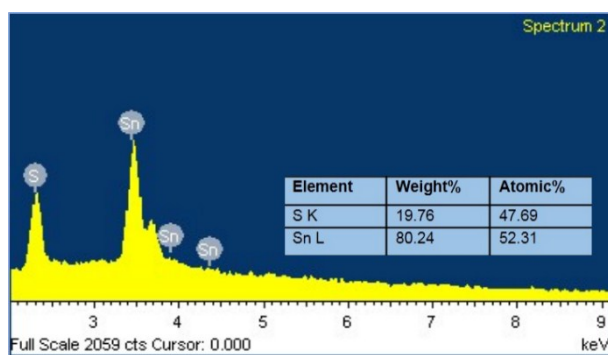


Fig S2. EDS characterization of SnS nanopyrramids.

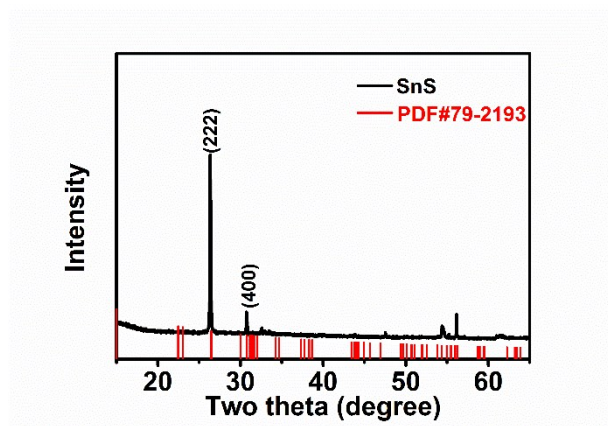


Fig S3. XRD pattern of SnS nanopyrramids.

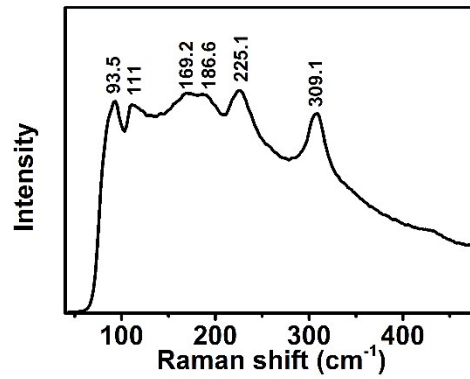


Fig S4. Raman spectrum of SnS nanopyramids.

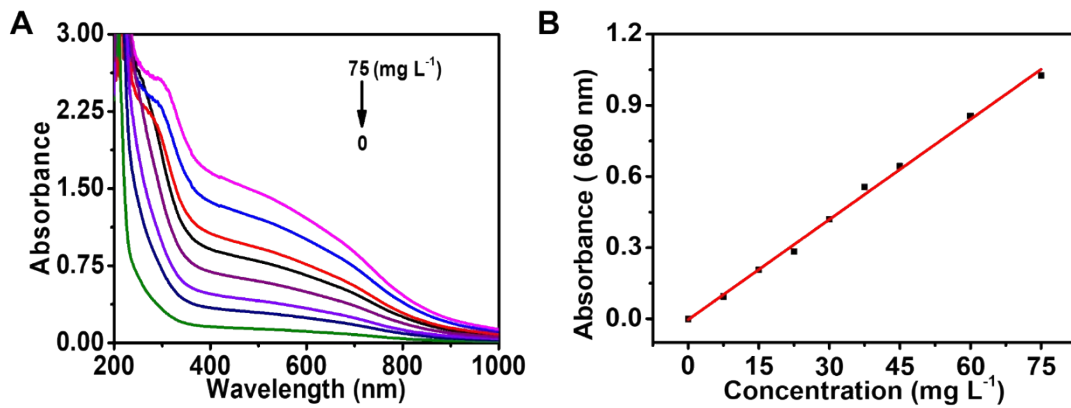


Fig S5. (a) UV-vis-NIR absorption spectra of SnS nanopyramids with a series of concentrations (7.5, 15, 22.5, 30, 37.5, 45, 60, and 75 mg L<sup>-1</sup>). (b) The plot of absorbance at 660 nm versus the concentration of SnS nanopyramids.

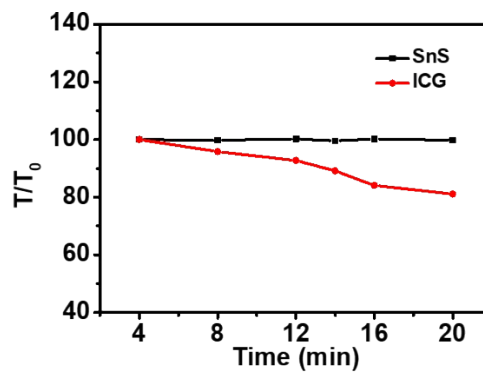
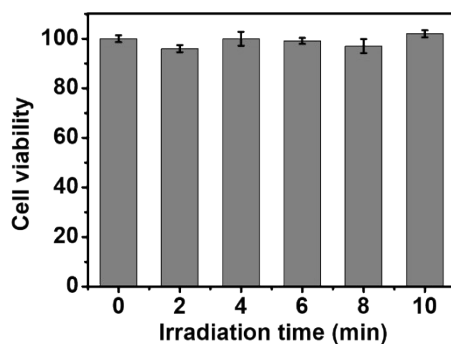
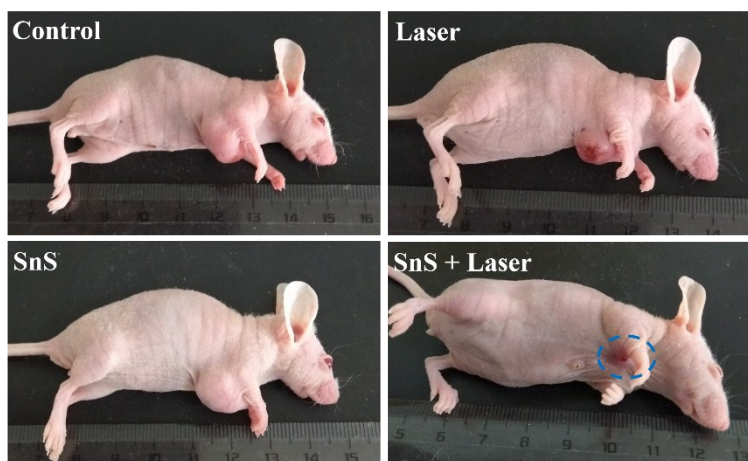


Fig S6. Photothermal stability of SnS nanopyramids under the irradiation of 660 nm at a power density of 1.2 W for 20 min.  $T_0$  is the highest temperature of sample under laser irradiation, and  $T$  is the temperature of sample at different time intervals after continuous laser irradiation.



**Fig S7.** Cell viability of *HeLa* cell irradiated with 660 nm laser ( $1.2 \text{ W cm}^{-2}$ ) for different time.



**Fig S8.** Representative images of the *HeLa* tumor bearing mice were taken after a series of treatments for two weeks.

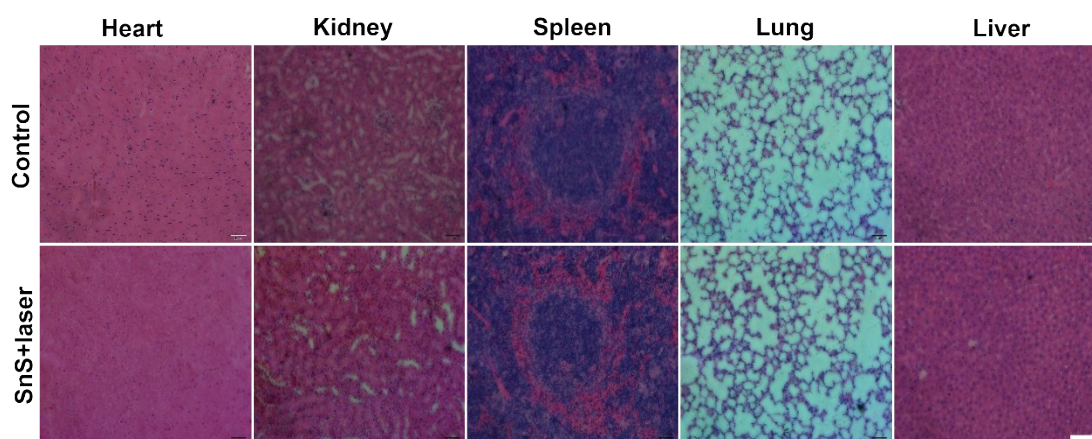


**Fig S9.** Hematoxylin and eosin stained tissue sections from mice injected with  $25 \mu\text{L}$  of PBS ( $\text{pH}=7.4$ ,  $10 \text{ mM}$ ) or SnS nanopyrramids solution ( $2 \text{ mg mL}^{-1}$ ) for 1 d (scale bar:  $100 \mu\text{m}$ ).

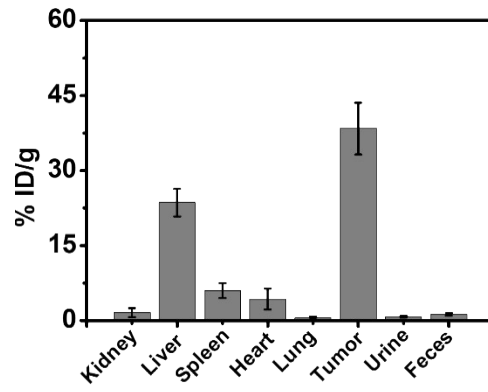


**Fig S10.** Biodistribution of SnS nanopyrramids in *HeLa* tumor-bearing ( $\sim 60 \text{ mm}^3$ ) female nude mice at 24 h after intratumoral injection.

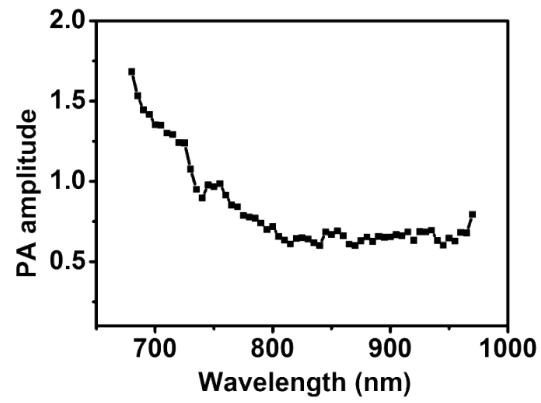


**Fig S11.** PA spectrum of SnS nanopyrramids.